

# Similaritons Formation in Synchronously Pumped Singly Resonant Optical Parametric Oscillators

Fuyong Wang,<sup>1,\*</sup> Guoqiang Xie,<sup>1,†</sup> Peng Yuan,<sup>1</sup> Liejia Qian,<sup>1</sup> and Dingyuan Tang<sup>2</sup>

<sup>1</sup>Key Laboratory for Laser Plasmas (Ministry of Education),  
Department of Physics and Astronomy, Shanghai Jiao Tong University, Shanghai, 200240, China

<sup>2</sup>School of Electrical and Electronic Engineering,  
Nanyang Technological University, Singapore 639798, Singapore

(Dated: April 22, 2019)

Similaritons is theoretically predicted in singly resonant optical parametric oscillators by numerical simulations. Self-similar solutions of coupled-wave equations is analysed by reducing coupled-wave equations to nonlinear Schrödinger equation. Parabola-like temporal intensity profile pulses evolution in opo is presented. Self-similar pulses with linear chirp have many practical and potential applications.

Self-similarity is an important nonlinear physical phenomenon and a hot topic in optics. In recent years, self-similarity has attracted much attention, including pulse evolution in an all-normal-dispersion lasers[1], optical fiber amplifiers[2, 3], fiber lasers[4] and mode-locked bulk lasers[5]. Optical similariton, which was first observed in a fiber laser[6], is a shape-preserving wave with its parameters such as amplitude and width varying with system parameters. Similariton is described by the self-similar solution of the inhomogeneous nonlinear Schrödinger equation (INLSE). Self-similar pulses in the optical fiber amplifiers[2] are asymptotic similaritons which are asymptotic solutions of governing equation. The pulses in these systems are growing self-similarly when entering self-similar region[2, 7]. Another type of optical similaritons are the exact solitonic similaritons and they are described by exact soliton solutions[8–11].

Parabolic intensity profile and linear chirp are the typical characteristics of optical similaritons. The analytical solutions of INLSE with time-independent gain can be generally obtained by self-similar transformation[2, 3, 7]. When the gain is time-dependent, it is difficult to obtain the analytical solutions of similaritons. It is found that the similaritons could be formed in passively mode-locked Ta:sapphire laser[5], where time-dependent gain or loss is included in INLSE. In general, similaritons could be formed in a nonlinear system including dispersion, nonlinearity and gain, providing they meet a certain relation. Since dispersion, nonlinearity and gain are also present in OPO, it is natural to ask whether similaritons or similariton-like pulses can be formed in OPO.

Despite substantial research about similaritons in many fields, similaritons or similariton-like pulses in OPO have never been reported. The analysis of the existence of similaritons in OPO has wide-ranging practical applications, such as pulse compression and generation of mid-infrared few-cycle pulses. The technique of generating similaritons in an OPO can support the generation femtosecond pulses by picosecond pulse pumping, and will significantly reduce the synchronization requirement in comparison with femtosecond OPOs. Physically, similariton in OPO means a new solution of three-wave coupled equations and a new type of optical pulse shaping in OPO.

In this letter we reduce the three-wave coupled equations to standard INLSE by rational approximation. We also numerically solve the three-wave coupled equations and obtain the similariton-like solution. Besides, the conditions of similariton formation in OPO are analyzed.

The equations describing OPO can be transformed to a frame of reference moving with velocity  $v_{gs} = 1/\frac{\partial k_s}{\partial \omega}$  by use of coordinate  $T = t - z/v_{gs}$ . Then the three-wave coupled equations for perfect phase matching ( $\Delta k = 0$ ) are[12]

$$i\frac{\partial E_s}{\partial z} + \gamma|E_s|^2 E_s - \frac{1}{2}\frac{\partial^2 k_s}{\partial \omega^2}\frac{\partial^2 E_s}{\partial T^2} = -\Gamma_s E_p E_i^*, \quad (1)$$

$$i\frac{\partial E_i}{\partial z} + i\left(\frac{\partial k_i}{\partial \omega} - \frac{\partial k_s}{\partial \omega}\right)\frac{\partial E_i}{\partial T} - \frac{1}{2}\frac{\partial^2 k_i}{\partial \omega^2}\frac{\partial^2 E_i}{\partial T^2} = -\Gamma_i E_p E_s^*, \quad (2)$$

$$i\frac{\partial E_p}{\partial z} + i\left(\frac{\partial k_p}{\partial \omega} - \frac{\partial k_s}{\partial \omega}\right)\frac{\partial E_p}{\partial T} - \frac{1}{2}\frac{\partial^2 k_p}{\partial \omega^2}\frac{\partial^2 E_p}{\partial T^2} = -\Gamma_p E_i E_s, \quad (3)$$

where  $E_{s,i,p}$  represent signal, idler and pump field and  $\frac{\partial^2 k_{s,i,p}}{\partial \omega^2}$  are their group-velocity dispersions (GVD), respectively.  $\frac{\partial k_{i,p}}{\partial \omega} - \frac{\partial k_s}{\partial \omega}$  represent group-velocity mismatches (GVM) of idler field and pump field relative to signal field. The second order nonlinear coefficients are given by:  $\Gamma_{s,p,i} = \frac{2\pi d_{eff}}{\lambda_{s,p,i} n_{s,p,i}}$ . Here  $d_{eff}$  is an effective second-order nonlinear coefficient.  $\lambda_{s,p,i}$  and  $n_{s,p,i}$  are wavelengths and refractive indices, respectively. Considering only the signal wave is resonant in the cavity, it only needs to take into account self-phase modulation evoked by third-order nonlinear effects of signal pulses. The parameter of the third-order nonlinearity on the signal field is expressed by,  $\gamma = (\pi/\lambda_s)(c\epsilon_0 n_s)n_2$ , where  $n_2$  is the intensity-dependent refractive index coefficient.

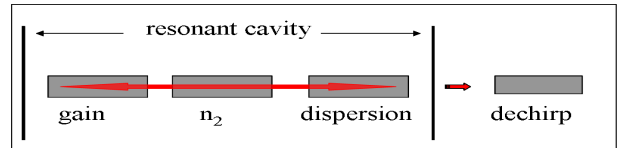


FIG. 1. Schematic of a singly resonant OPO generating similariton-like pulses.

If the nonlinear crystal length is much shorter than both the walk-off lengths and the dispersion lengths afforded by the crystal for the idler and the pump, then we neglect the GVM and GVD of idler and pump waves. Because the gain of OPO is small and the crystal length is very short, small change of the signal field occurs during each one round trip. Especially, the signal field can be approximately taken as a constant when it reaches saturation. Hence, we assume  $E_s$  is constant over a single round trip when dealing with Eq.(2),(3). Thus, we obtain

$$\frac{\partial^2 E_i}{\partial z^2} + a^2 E_i = 0, \quad (4)$$

$$\frac{\partial^2 E_p}{\partial z^2} + a^2 E_p = 0. \quad (5)$$

Here,  $a = \sqrt{\Gamma_i \Gamma_p |E_s|^2}$ . Using the initial idler field  $E_i(0) = 0$ , we obtain the expression of idler field:  $E_i = i \Gamma_i E_p(0) E_s^* \sin(az)$ . Likewise, using the initial pump field  $E_p(0)$ , we obtain the pump field:  $E_p = E_p(0) \cos(az)$ . As a consequent, the right part of Eq.(1) can be reduced to

$$-\Gamma_s E_p E_i^* = i \Gamma_s \Gamma_i |E_p(0)|^2 \frac{\sin(2az)}{2a} E_s. \quad (6)$$

Therefore, the governing equations of the signal field  $E_s$  in OPO can be reduced to the standard INLSE:

$$i \frac{\partial E_s}{\partial z} = \frac{1}{2} \beta_2 \frac{\partial^2 E_s}{\partial T^2} - \gamma |E_s|^2 E_s + i \frac{g}{2} E_s, \quad (7)$$

where,  $g = \Gamma_s \Gamma_i |E_p(0)|^2 \frac{\sin(2az)}{a}$  is parametric gain. Here,  $\beta_2 = \frac{\partial^2 k_s}{\partial \omega^2}$  is group velocity dispersion for signal field and  $\gamma = (\pi/\lambda_s)(c\epsilon_0 n_s) n_2$  represents third-order nonlinear parameter.

The schematic of singly resonant OPO is showed in Fig. 1. We numerically solve Eqs.(1),(2) and (3) by using split-step Fourier algorithm. In the simulation, we assume the signal pulse is perfectly synchronized with the pump pulse at the entrance of the crystal. The OPO cavity boundary conditions are:  $E_s(n+1) = r_s E_s(n)$ ,  $E_p(n+1) = E_p$  and  $E_i(n+1) = 0$ , where  $n$  represents the  $n$ th round trip and  $r_s$  is the field reflectivity for signal field with a value of  $r_s = \sqrt{0.98}$ . We use KTA as nonlinear crystal, with  $n_2 = 1.7 \times 10^{-19} \text{ m}^2/\text{W}$  and  $d_{eff} = 2.04 \text{ pm/V}$ . The wavelength of pump pulse is  $\lambda_p = 1064 \text{ nm}$  and its pulse duration is  $10 \text{ ps}$ . We choose  $\lambda_s = 3300 \text{ nm}$ ,  $\lambda_i = 1570.3 \text{ nm}$  as signal and idler wavelength, respectively. The value of  $\gamma\beta_2$  must be positive for formation of self-similariton[3, 7]. Owing to the nonlinear parameter  $\gamma > 0$ , we need insert a positive dispersive device to offset the negative dispersion of KTA crystal and make the net dispersion in the cavity is positive at signal wavelength. The length of KTA nonlinear crystal is taken as  $1 \text{ mm}$ , which provides a dispersion of  $-480 \text{ fs}^2$  at  $3.3 \mu\text{m}$  wavelength. One can insert a Ge plate in the cavity, which provides a dispersion of  $+1427 \text{ fs}^2/\text{mm}$  at  $3.3 \mu\text{m}$ , to realize the required positive net intracavity dispersion. The expression of walk-off length is  $L_w = T_0/GVM$ , where  $T_0$  is the

pump pulse duration. In our simulation, the GVM values of pump field and idler field relative to signal field are  $3.33 \text{ fs/mm}$  and  $43.33 \text{ fs/mm}$  for KTA crystal, respectively. We calculate walk-off lengths of pump and idler fields relative to signal field to be  $3003 \text{ mm}$ ,  $230 \text{ mm}$ , respectively. In the simulation we assume the pump pulse has a Gaussian temporal profile.

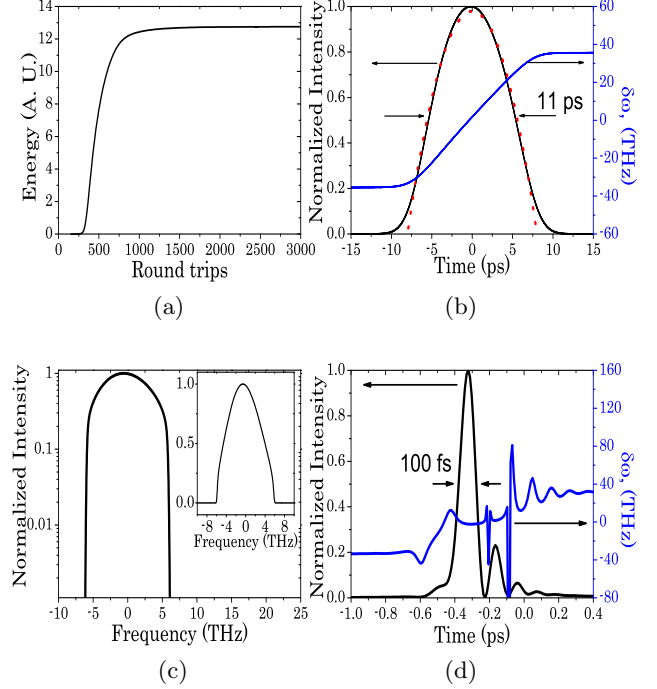


FIG. 2. Results of numerical simulations. (a) The evolution of signal pulse energy with round-trip number in the cavity. (b) Temporal intensity profile (black solid curve), instantaneous frequency (blue solid curve), and the parabolic fit (dotted curve) to intensity profile for signal pulse. (c) Signal pulse spectrum on semilog scale. Inset: spectrum on linear scale. (d) Dechirped pulse intensity profile (black solid curve) and instantaneous frequency (blue solid curve).

The evolution of signal pulse energy is illustrated in Fig. 2(a). In the simulation, a quantum noise signal with random phase is used as the initial signal field. As the number of the round trips increases, the signal pulse energy becomes larger and larger, finally reaches a saturation state. Figure. 2(b) shows the output temporal intensity profile and instantaneous frequency of the signal pulse when it reaches saturation state. As similariton observed in fiber laser[6], the temporal intensity profile of signal pulses has an approximately parabolic shape and the signal pulse chirp is linear across the pulse. In the simulation, we find that the slope of linear chirp is inversely proportional to the net intracavity dispersion, which is consistent with the similariton evolution in the fiber laser.

Figure. 2(c) shows the corresponding spectrum of signal pulse with unique shape: parabolic near the peak with a transition to a steep decay, which is the typical characteristic of similaritons[6, 13]. Since the temporal intensity profile, spectral shape and the linear chirp characteristic of the signal pulses are identical with those

of similaritons, we believe formation of similariton-like pulse in the singly resonant OPO.

Since the linear chirp facilitates efficient pulse compression, we can dechirp the signal pulse outside the cavity and obtain a femtosecond compressed pulse. According to our simulation, a negative dispersion of  $-2.14 \times 10^5 \text{ fs}^2$  is required to dechirp the pulse, and a bulk Bragg grating can conveniently provide the required dispersion. After dechirping, we obtain a 110-fold compression from the 11-ps chirped pulses. The compressed pulse has a pulse duration as short as 100 fs, which corresponds to  $\sim 10$  optical cycles for signal pulses at  $3.3 \mu\text{m}$  wavelength. Figure. 2(d) illustrates the compressed signal pulse characteristics. The compressed signal pulse includes trailing satellite pulses and remains nonlinear chirp, which are found to be caused by the GVMs between three waves. We also numerically simulated the compressed signal pulse and its chirp characteristics without taking into account GVMs, and in this case the trailing satellite pulses disappear and the instantaneous frequency becomes constant across the pulse. Thus, in order to achieve clean compressed pulses, the GVMs between three waves should be as small as possible in OPO.

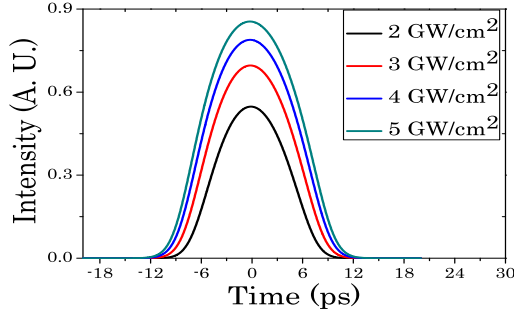


FIG. 3. Temporal intensity profile of signal pulse for different pump intensities.

As similaritons in fiber lasers, the similariton-like pulses in OPO can endure high energy propagating in the cavity without pulse collapse. The amplitudes and widths of the signal field increase with the intensity of the pump pulse, as shown in Fig. 3. The energy of pump pulse is a system parameter that determines the signal pulse characteristics. In addition, by the simulation we also find, when the pump intensity is too strong or the nonlinear crystal is very long, the gain given in Eq.(7) will oscillate along the crystal and finally the similariton-like pulses cannot be formed in the OPO. Thus, appropriate pump intensity and nonlinear crystal length are required for formation of similariton-like pulses in the OPO.

Figure. 4 exhibits the influence of net intracavity dispersion on the signal pulse spectrum. A certain amount of dispersion is required for formation of similariton-like pulses in OPO. Too small value of dispersion fails to form stable similariton-like pulses in the cavity. In our case, the value of dispersion should be greater than

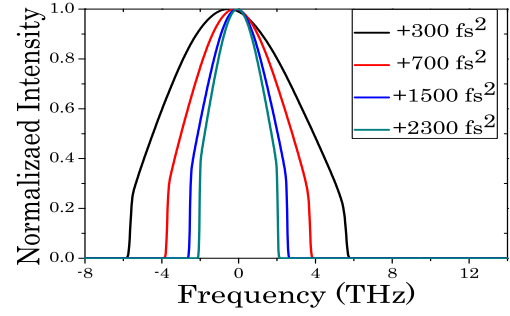


FIG. 4. Spectral profile of signal pulse for different values of net intracavity dispersion with intensity-dependent refractive index coefficient  $n_2 = 1.7 \times 10^{-19} \text{ m}^2/\text{W}$ .

$\sim +100 \text{ fs}^2$  and the dispersion region allowing the generation of similariton-like pulses is very wide. However, large value of dispersion will narrow the phase matching bandwidth in OPO, which in turn leads to a narrow signal pulse spectrum and prevents effective pulse compression. Therefore, the value of net intracavity dispersion must be appropriate for formation of wideband similariton-like pulses in OPO.

It has been shown that soliton pulses can be formed in singly resonant OPO[14], where the negative intracavity dispersion is balanced with positive third-order nonlinearity. However, in our simulation we find the net intracavity dispersion must be positive for formation of similariton-like pulses in OPO with positive nonlinearity parameter; and negative net intracavity dispersion is required for forming similariton-like pulses in OPO with negative nonlinearity. That is to say the sign of dispersion must be the same as that of nonlinearity, namely  $\gamma\beta_2 > 0$ , which is the requirement of forming similaritons in nonlinear optical system[3, 7]. It is known that intensity-dependent refractive index coefficient  $n_2$  determines the nonlinearity amount. The parameter  $n_2$  in our case is about six times as large as that in Ref.[14]. INLSE is known to have similariton and soliton solutions, and the formation of similariton in OPO depends on a certain group of system parameters.

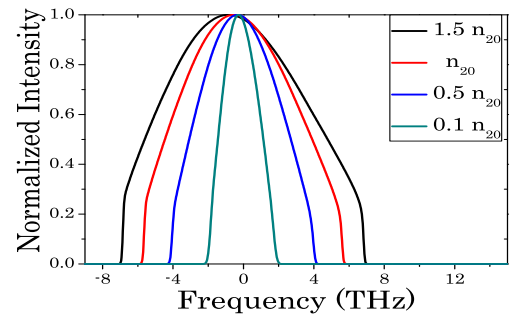


FIG. 5. Spectral profile of signal pulse for different intensity-dependent refractive index coefficients  $n_2$  with the value of net intracavity dispersion:  $300 \text{ fs}^2$  ( $n_{20} = 1.7 \times 10^{-19} \text{ m}^2/\text{W}$ ).

The intensity-dependent refractive index coefficient  $n_2$  plays an important role in the formation of similariton-like pulses in OPO. Figure. 5 shows the characteristics of signal pulse spectra with different  $n_2$  values and the results show larger  $n_2$  value supports broader signal pulse spectrum. It can be easily understood that the nonlinearity will serve as self-phase modulation and effectively broaden the signal pulse spectrum. Finally, the spectrum broadening due to nonlinearity and the spectrum narrowing due to dispersion will reach to balance, which commonly determine the spectral width of signal pulse. It is worthwhile to note that the case here is distinct to the traditional soliton lasers, where the balance between nonlinearity and dispersion leads to a temporal soliton pulse and generally  $\gamma\beta_2 < 0$  is required.

The physical process of three waves coupling in OPO is more complicated than that of fiber lasers and amplifiers. In the OPO, the GVMs between the three waves have a negative effect on the formation of similariton-like pulses. Large GVMs between the three waves will lead to nonlinear chirp in signal pulses and even result in signal pulse collapse in OPO. Therefore, GVMs between the three waves should be as small as possible for the formation of similariton-like pulses in OPO. In addition, since long pump pulse duration will increase the walk-off lengths and dispersion lengths, long pump pulse will reduce the effects of GVM and dispersion on the formation of similariton-like pulses in OPO.

According to above analysis, the formation of similariton-like pulses in OPO requires three main conditions. Firstly, the value of  $\gamma\beta_2$  must be positive. That is to say, the sign of net intracavity dispersion must be the same as that of the nonlinearity parameter. Secondly, the GVMs between three waves should not be too large. Thirdly, the intensity-dependent refractive index coefficient  $n_2$  and net intracavity dispersion should have moderate values.

In conclusion, we have theoretically studied the formation of similariton-like pulses in singly resonant OPO. The numerical simulation results show that with appropriate system parameters in OPO, more than 110-fold compression and cycle-level ultrashort pulses can be achieved by picosecond pulse pumping. The similariton-like OPO will have great potential applications for pulse

compression and mid-infrared few-cycle pulses generation. To the best of our knowledge, this is the first theoretical prediction of formation of similariton-like pulses in OPO.

The work is partially supported by the National Natural Science Foundation of China (Grant No. 61008018 and 11121504) and the National Basic Research Program of China (Grant No. 2013CBA01505).

---

\* Also at Key Laboratory for Laser Plasmas (Ministry of Education), Department of Physics and Astronomy, Shanghai Jiao Tong University, Shanghai, 200240, China  
† xiegq@sjtu.edu.cn

- [1] William H. Renninger, Andy Chong, and Frank W. Wise, *Phys. Rev. A*, **82**, 021805 (2010).
- [2] V. I. Kruglov, A. C. Peacock, J. M. Dudley, and J. D. Harvey, *Opt. Lett.*, **25**, 1753 (2000).
- [3] M. E. Fermann, V. I. Kruglov, B. C. Thomsen, J. M. Dudley, and J. D. Harvey, *Phys. Rev. Lett.*, **84**, 6010 (2000).
- [4] Bulent Oktem, Coşkun Ülgüdür, and F. Ömer Ilday, *nature photonics*, **4**, 307 (2010).
- [5] F. Ö. Ilday, F. W. Wise, and F. X. Kaertner, *Opt. Express*, **12**, 2731 (2004).
- [6] F. Ö. Ilday, J. R. Buckley, W. G. Clark, and F. W. Wise, *Phys. Rev. Lett.*, **92**, 213902 (2004).
- [7] V. I. Kruglov, A. C. Peacock, and J. D. Harvey, *J. Opt. Soc. Am. B*, **19**, 461 (2002).
- [8] Sergey A. Ponomarenko and Govind P. Agrawal, *Phys. Rev. Lett.*, **97**, 013901 (2006).
- [9] V. I. Kruglov, A. C. Peacock, and J. D. Harvey, *Phys. Rev. Lett.*, **90**, 113902 (2003).
- [10] Sergey A. Ponomarenko and Govind P. Agrawal, *Opt. Lett.*, **32**, 1659 (2007).
- [11] Sergey A. Ponomarenko and Govind P. Agrawal, *Opt. Express*, **15**, 2963 (2007).
- [12] A. V. Smith, Russell J. Gehr, and Mark S. Bowers, *J. Opt. Soc. Am. B*, **16**, 609 (1999).
- [13] Junsong Peng, Li Zhan, Zhaochang Gu, Kai Qian, Shouyu Luo, and Qishun Shen, *Phys. Rev. A*, **86**, 033808 (2012).
- [14] Pey-Schuan Jian, William E. Torruellas, Marc Haelterman, Stefano Trillo, Ulf Peschel, and Falk Lederer, *Opt. Lett.*, **24**, 400 (1999).